CHEMISTRY
A EUROPEAN JOURNAL

DOI: 10.1002/chem.200902501

Determination of the Absolute Configuration of Pentacoordinate Chiral Phosphorus Compounds in Solution by Using Vibrational Circular Dichroism Spectroscopy and Density Functional Theory

Guochun Yang,[a] Yunjie Xu,*[a] Jianbo Hou,[b] Hui Zhang,[b] and Yufen Zhao*[b]

Abstract: Vibrational circular dichroism (VCD) spectroscopic measurements and density functional theory (DFT) calculations have been used to obtain the absolute structural information about four sets of diastereomers of pentacoordinate spirophosphoranes derived separately from L- (or D-) valine and L- (or D-) leucine for the first time. Each compound contains three stereogenic centers: one at the phosphorus center and two at the amino acid ligands. Extensive conformational searches for the compounds have been carried out and their vibrational absorption (VA) and VCD spectra have been simulated at the B3LYP/6-311++G** level. Although both VA and VCD spectra are highly sensitive to the structural variation of the apical axis, that is, the O–P–O or N–P–O arrangement, the rotamers generated by the aliphatic amino side chains show little effect on both. The dominant experimental VCD features in the 1100–1500 cm^{-1} region were found to be controlled by the chirality at the phosphorus center, whereas those at the C=O stretching region are determined by the chirality of the amino acid ligands. The good agreement between the experimental VA and VCD spectra in $CDCl_3$ solution and the simulated ones allows us to assign the absolute configurations of these pentacoordinate phosphorus compounds with high confidence. This study shows that the VCD spectroscopy complemented with DFT calculations is a powerful and reliable method for determining the absolute configurations and dominating conformers of synthetic phosphorus coordination complexes in solution.

Keywords: absolute configuration · amino acid ligands · density functional calculations · isomerization · vibrational spectroscopy

Introduction

Phosphorous plays a crucial role in stereoselective chemical syntheses and in biological systems.[1,2] Chiral organophosphorus ligands, for example, are of great importance in the development of asymmetric homogeneous catalysts. Pentacoordinate phosphorus compounds in particular have attracted much attention for their roles as intermediates or transition states in many biological processes such as enzymatic phosphoryl transfer reactions[3,4] and hydrolysis or formation of DNA, RNA, cyclic AMP (cAMP), and other biologically relevant phosphorous compounds.[5] Because their structural and dynamic properties are strongly related to the reactivity and/or selectivity of the processes involved, a good number of model pentacoordinate phosphorous compounds have been synthesized and characterized to aid our understanding. A wealth of information about apicophilicity, antiapicohilicity, and Berry pseudorotation has been obtained for these hypervalent phosphorus compounds.[6] Although knowledge about the stereochemistry, that is, the absolute configurations, of these compounds is essential in furthering our basic understanding of these important processes, very few absolute structural studies of pentacoordinate phosphorous complexes have been reported so far.[7,8]

One particularly interesting class of pentacoordinate phosphorous complexes is the class with amino acid residues as chiral chelate ligands. They are considered important intermediates in the self-assembly reactions of *N*-phospho-

[a] Dr. G. Yang, Prof. Dr. Y. Xu
Department of Chemistry, University of Alberta
Edmonton, AB, T6G 2G2 (Canada)
Fax: (+1) 780-492-8231
yunjie.xu@ualberta

[b] Prof. J. Hou, Prof. H. Zhang, Dr. Y. Zhao
Department of Chemistry
College of Chemistry and Chemical Engineering
and The Key Laboratory for Chemical Biology of Fujian Province
Xiamen University, Xiamen, 361005 (P.R. China)
Fax: (+86) 592-218-6292
E-mail: yfzhao@xmu.edu.cn

Supporting information for this article is available on the WWW under http://dx.doi.org/10.1002/chem.200902501.

amine acids into peptides.[9,10] In recent years, the synthesis and solid-state structural characterization (by using X-ray crystallography) of several pentacoordinate phosphorus compounds containing amino acid residues have been reported.[8,11,12] It is, however, often time consuming and sometimes impossible to obtain a single crystal for solid-state structural characterization.[8] Moreover, because most chemical reactions and biological processes occur in solution, it is of great interest to determine the absolute configurations of these hypervalent chiral phosphorus compounds in the solution phase.

Vibrational circular dichroism (VCD) spectroscopy measures the differential absorption of a chiral molecule with respect to the left- and right-handed circularly polarized radiation in the infrared region. It has emerged in recent years as a powerful analytical tool to provide structural information about absolute configurations and conformations of biomolecules[13] and chiral organic compounds.[14] In this report, the absolute configurations and dominating conformations of four sets of diastereomers of chiral pentacoordinate spirophosphoranes, derived from L- (or D-) valine , and L- (or D-) leucine (Scheme 1), have been determined by using VCD

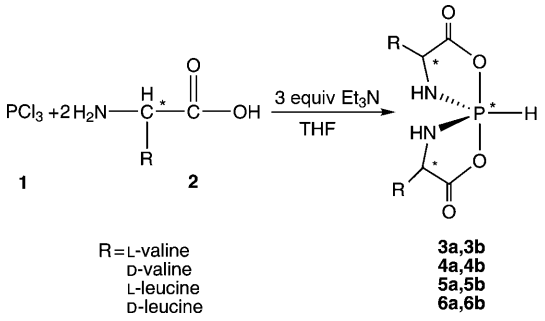

Scheme 1. The four pairs of diastereomers investigated in this paper.

spectroscopy in conjunction with density functional theory (DFT) calculations. These compounds were synthesized with the route shown in Scheme 1 and the separation of the diastereoisomers **a** and **b** was performed by using reverse-phase HPLC with a TC-C_{18} column.[12] To the best of our knowledge, no structural determination by using VCD spectroscopy has been previously applied to pentacoordinate phosphorus compounds. The study here shows that the VCD spectroscopy complemented with DFT calculations is a powerful method for determining the absolute configurations and dominating conformers of synthetic phosphorus coordination complexes that are difficult to crystallize.

Results and Discussion

The pentacoordinate phosphorous compounds investigated were synthesized by using the method outlined in Scheme 1 and are described in detail in Ref. [12]. The separation of the diastereoisomers **a** and **b** was performed by using reverse-phase HPLC with a TC-C_{18} column. The solubility testing, retention time, ^{31}P NMR data, and circular dichroism (CD) data obtained indicate that **3a**/**4a**, **3b**/**4b**, **5a**/**6a**, and **5b**/**6b** are pairs of enantiomers. The X-ray crystallography of **3a**/**4a** confirmed that they indeed are a pair of enantiomers.[12] On the other hand, **a** and **b** are a pair of diastereomers (Scheme 1), and **a** generally has a higher solubility than **b**. The reported HPLC analysis showed that every isomer was obtained with an enantiopurity of 99 %.[12]

To explore the application of vibrational absorption (VA) and VCD spectroscopy for pentacoordinate phosphorus compounds, we carried out experimental measurements and DFT calculations for all of the products shown. The experimentally obtained VA and VCD spectra for **3a**, **3b**, **5a**, and **5b** are given in Figure 1. The corresponding VA and the VCD spectra for the corresponding enantiomers **4a**, **4b**, **6a**, and **6b** are the same or of opposite signs, respectively. As can be seen, the VA spectra shown in Figure 1 are nearly identical for the **a** and **b** diastereomers. It is not possible to tell them apart by using VA spectroscopy alone. Their corresponding VCD spectra, on the other hand, show substantial differences in the frequency region below 1500 cm^{-1}, suggesting that it may be possible to use VCD spectroscopy to differentiate between the two different diastereomers. Also

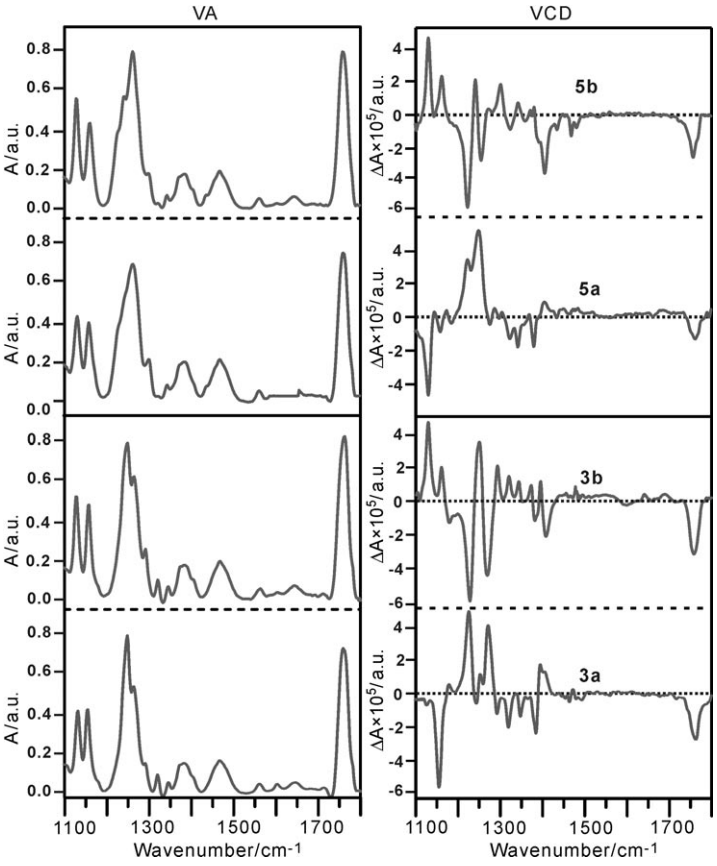

Figure 1. The experimental VA and VCD spectra of the compounds **3a**, **3b**, **5a**, and **5b**.

note that replacing the chiral amino acid ligand valine with leucine makes hardly any noticeable changes in the VA spectra, whereas there are some changes in the corresponding VCD spectra.

In the following, we describe the theoretical searches for possible isomers. The corresponding VA and VCD spectra have been simulated for comparison with the experimental data. We will evaluate how VA and VCD spectroscopy can be used to characterize the isomerism and absolute configurations of pentacoordinate phosphorus compounds. The absolute configuration assignments achieved with VCD spectroscopy will be compared to those determined by using X-ray crystallography whenever available. As mentioned before, the two isomers of **3** are enantiomers to the corresponding isomers of **4**, and the same relationship holds for the isomers of **5** and **6**. Therefore, we describe only our treatment of **3** and **5** in the following discussions for simplicity.

Pentacoordinate phosphorus compounds 3 and 4: The pentacoordinate phosphorous compounds, in principle, can take on trigonal bipyramidal (TBP) and square/rectangular pyramidal (SP) geometry. In the majority of cases, the slightly distorted TBP geometry is favored.[6] We have performed preliminary calculations on **3** and found that the molecule takes on TBP geometry at the potential minima, whereas an identified transition state (see below) has SP geometry. This is consistent with the X-ray crystal structure obtained for **3**, which has TBP geometry. Therefore, we have focussed on the TBP conformers in the subsequent search for possible stereoisomers.

Pentacoordinate phosphorus compound **3** has three stereogenic centers: one of them is the phosphorus atom, and the other two are at the amino acid ligands. This produces four pairs of diastereomers, $\Lambda_p SS$ and $\Delta_p RR$, $\Lambda_p SR$ and $\Delta_p RS$, $\Lambda_p RS$ and $\Delta_p SR$, and $\Lambda_p RR$ and $\Delta_p S$, in which the two isomers in each pair are mirror images of each other. We, therefore, only need to consider the $\Lambda_p SS$, $\Lambda_p SR$, $\Lambda_p RS$, and $\Delta_p SS$ types in the structural search because the corresponding VCD spectra of the rest of four are just mirror images of these four. Because only enenatiomerically pure amino acids were used in the synthetic reactions, it would be expected to have only *RR* or *SS* configurations for the resulting complexes. To investigate how the chirality of the different stereogenic centers influences the appearance of the VCD spectra, we still included the calculations for the possible *SR* or *RS* stereoisomers.

In addition, a large number of possible structural isomers exist, which may be in different conformations. First, we consider the different arrangements of ligand binding sites on the apical axis. For example, compound **3** can have an O–P–O, N–P–O, N–P–N, O–P–H, or N–P–H apical axis. The DFT calculations performed show that the N–P–N conformation of compound **3** is not a minimum and that the O (or N)–P–H conformations are significantly less stable ($\approx$17 kcal mol^{-1}) than the others considered here. The O–P–O and N–P–O types were found to be minima, consistent with the previous experimental observation that the pentacoordinate phosphorus compounds mainly exist as O–P–O and N–P–O type conformers, and that the N–P–N type has rarely been detected.[6] Combining this consideration with the chirality consideration described above, we expect to have three kinds of O–P–O and four kinds of N–P–O stereoisomers. There are only three kinds of O–P–O stereoisomers because $\Lambda_p SR$ and $\Lambda_p RS$ are the same in this case as the two bidentate amino acid ligands are identical.

Another further consideration is that the valine ligand can itself exist in different conformations. A conformational search for valine itself has been previously reported.[15] The conformational consideration can be separated into two categories: the first one is related to the amino acid fragment, and the second one is related to the rotation of the aliphatic side chain $CH(CH_3)_2$ (Figure 2). In the complexes studied here, the amino acid fragment is locked into one particular conformation because of the coordination bonds to the P center. The rotation around the two C–C bonds indicated in

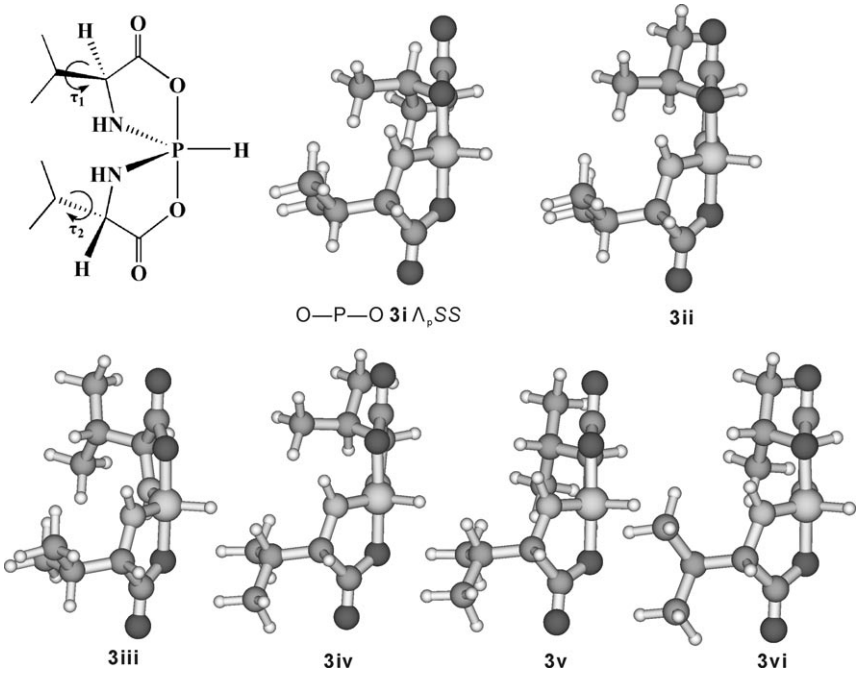

Figure 2. The rotations of the aliphatic side chain of valine and the optimized geometries of the six lowest energy O–P–O-type $\Lambda_p SS$ conformers of **3** at the B3LYP/6-311++G** level of theory.

Figure 2, on the other hand, can generate more possible conformers. Indeed, three different conformations have been identified here for each side chain, similar to that reported for the valine monomer.[15a]

For the O–P–O $\Lambda_p SS$-type structures the valine side chain can in principle generate nine conformers. But a closer look reveals that three of them are redundant because the two bidentate ligands are the same and both bind to P with the oxygen atoms at the axial positions. Indeed, all six proposed conformational geometries were confirmed to be minima by the geometry optimization and the subsequent harmonic frequency calculations. These six geometries **3i–3vi** are given in Figure 2. Their calculated relative total energies ΔE, relative Gibbs free energies ΔG, and the normalized Boltzmann factors B_f at 298.15 K based on the relative Gibbs free energy and total energy are listed in Table 1. Among these six conformers, **3i** is the most stable one, which contains two secondary C–H···O-type hydrogen bonds with a bond length of 2.71 Å. The calculated VA and VCD spectra of **3i–3vi** are presented in Figure 3. The main signatures of both VA and VCD spectra appear to be quite similar for all six conformers. It is not surprising that the VA spectra are indifferent to the side-chain conformations because the vibrational frequencies and intensities are rarely altered by such subtle changes. VCD spectra, on the other hand, are often quite sensitive to changes in dihedral angles and have been extensively used to tell different conformers apart.[16] In this particular case, the different orientations of the two $CH(CH_3)_2$ side chains appear to have only minor a influence on the VCD spectra.

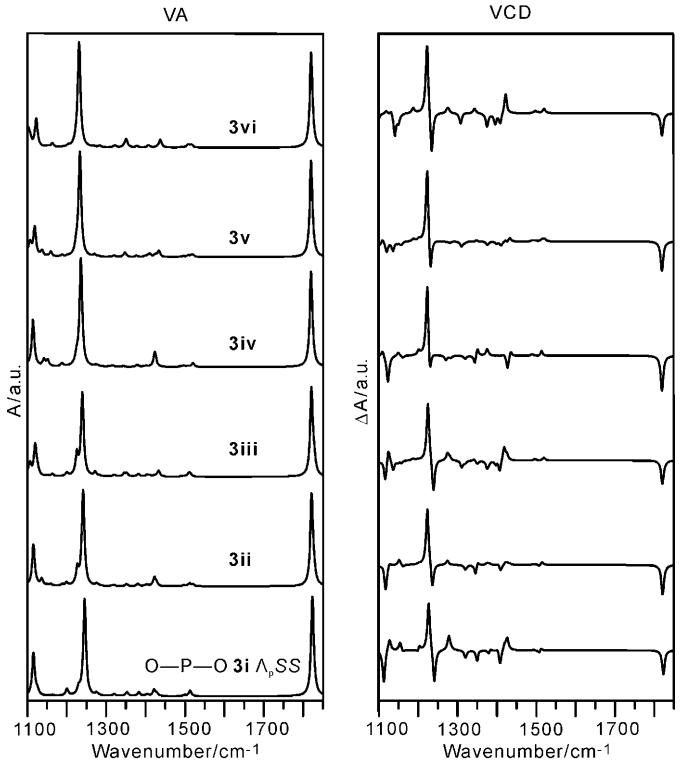

Figure 3. The calculated VA and VCD spectra of the six O–P–O-type $\Lambda_p SS$ conformers of **3** at the B3LYP/6-311++G** level of theory.

Table 1. The relative Gibbs free energies ΔG (kcal mol^{-1}), relative total energies ΔE (kcal mol^{-1}), and the normalized Boltzmann factors B_f (in %) at 298.15 K based on the relative Gibbs free energy and the relative total energy of the isomers of **3** at the B3LYP/6-311++G** level of theory.

Monomer	ΔG	$B_f(\Delta G)$	ΔE	$B_f(\Delta E)$
		O–P–O conformers		
3i $\Lambda_p SS$	0.0[a]	69.67	0.0	63.83
3ii	1.42	6.37	0.88	14.45
3iii	0.84	16.98	0.96	12.72
3iv	2.02	2.28	1.58	4.41
3v	1.89	2.89	1.78	3.14
3vi	2.17	1.80	2.24	1.45
3i $\Lambda_p SR$	0.0	46.37	0.0	50.27
3ii	0.69	14.38	0.73	14.77
3iii	1.15	6.66	1.22	6.39
3iv	0.67	14.97	0.80	12.92
3v	1.37	4.60	1.49	4.09
3vi	1.82	2.16	1.99	1.75
3vii	1.07	7.62	1.19	6.77
3viii	1.80	2.22	1.88	2.09
3ix	2.26	1.02	2.35	0.95
3i $\Delta_p SS$	0.00[b]	58.99	0.00	60.34
3ii	0.93	12.24	1.12	9.15
3iii	0.64	19.93	0.62	21.07
3iv	1.92	2.31	2.25	1.34
3v	1.75	3.10	1.82	2.79
3vi	1.69	3.43	1.44	5.32
		N–P–O conformers		
3i $\Lambda_p SS$	1.66	–	1.85	–
3i $\Lambda_p SR$	1.34	–	1.56	–
3i $\Lambda_p RS$	0.97	–	1.08	–
3i $\Lambda_p RR$	0[c]	–	0	–

[a] O–P–O **3i** $\Lambda_p SS$ is 0.33 kcal mol^{-1} higher than O–P–O **3i** $\Lambda_p SR$. [b] O–P–O **3i** $\Delta_p SS$ is 0.23 kcal mol^{-1} higher than O–P–O **3i** $\Lambda_p SR$. [c] N–P–O **3i** $\Lambda_p SS$ is 14.66 kcal mol^{-1} higher than O–P–O **3i** $\Lambda_p SR$.

By using the same procedure described for $\Lambda_p SS$, we obtained the six most stable O–P–O $\Delta_p SS$ conformers. Their geometries are given in Figure S1 in the Supporting Information. Conformer **3i** $\Delta_p SS$ is the most stable of the $\Delta_p SS$ conformers and has two secondary C–H···O hydrogen bonds, the bond lengths of which are about 2.73 Å. The calculated results of the $\Delta_p SS$ conformers are also provided in Table 1. The calculated VA and VCD spectra of **3i–3vi** $\Delta_p SS$ are presented in Figure 4. Just as for the $\Lambda_p SS$ conformers, the main VCD signatures are more or less the same among the six conformers, suggesting that the more subtle changes in the orientations of the two $CH(CH_3)_2$ side chains have little effect on the appearance of the VCD spectra. The C=O stretching signals are again negative for all six $\Delta_p SS$ conformers, just as for the $\Lambda_p SS$ conformers. The main VCD features at 1250 cm^{-1}, on the other hand, are of opposite signs of those of $\Lambda_p SS$. This indicates that the chirality of the ligands mainly controls the C=O stretching VCD sign, whereas the chirality of the phosphorous center has a controlling effect on the dominant VCD features between 1100–1500 cm^{-1}. It is interesting to note that the experimentally previously reported observed CD spectra[12] show that the sign of the CD peaks is determined by the chirality of

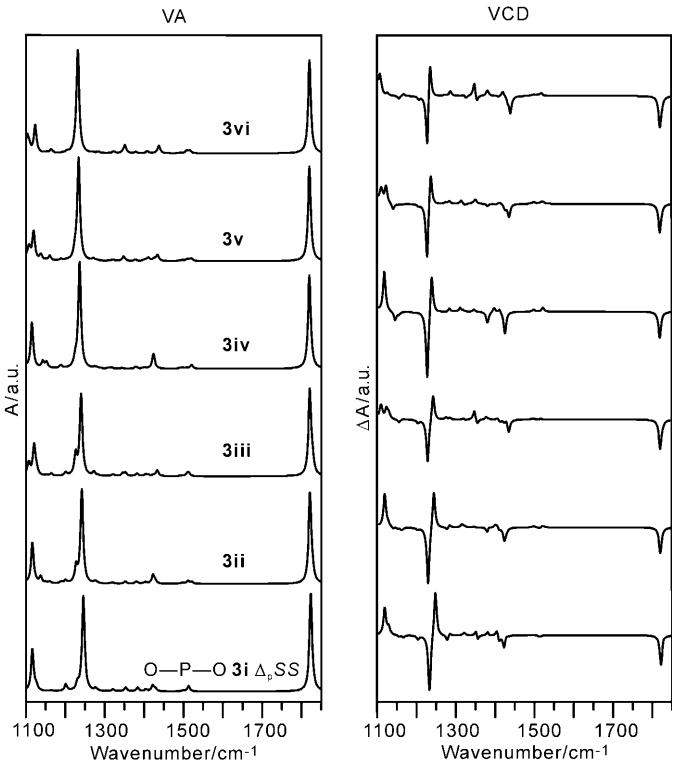

Figure 4. The calculated VA and VCD spectra of the six O–P–O type $\Delta_p SS$ conformers of **3** at the B3LYP/6-311++G** level of theory.

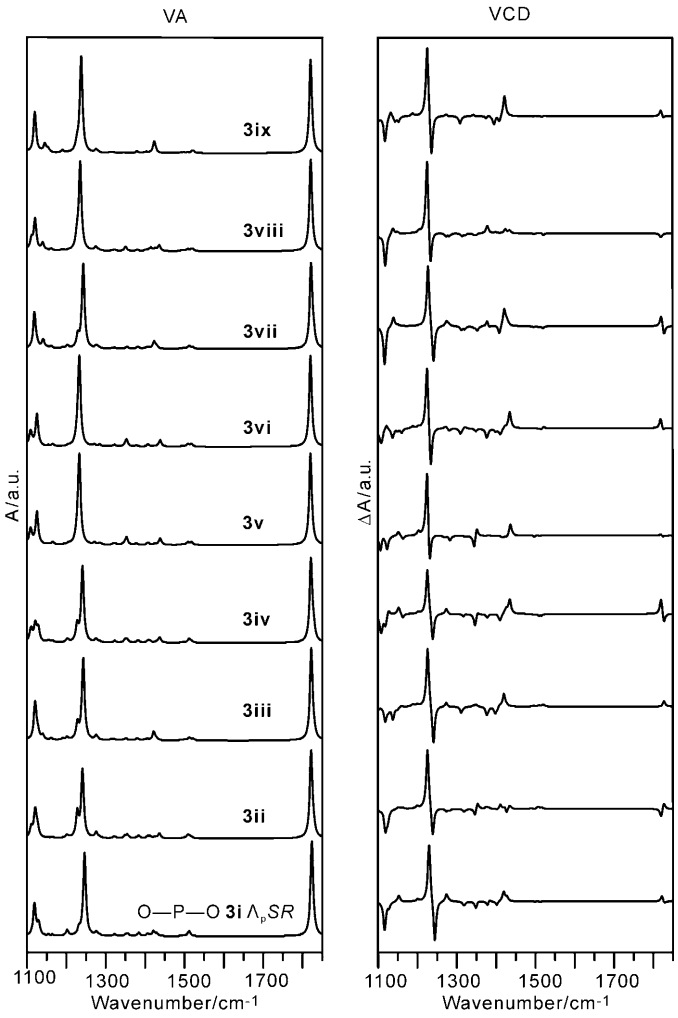

Figure 5. The calculated VA and VCD spectra of the nine O–P–O $\Lambda_p SR$ conformers of **3** at the B3LYP/6-311++G** level of theory.

the phosphorous center and is independent of the chirality of the ligands. This can be understood because the valine side chain is not chromogenic. So the VCD spectra reported here can provide not only information about the chirality of the P center but also about that of the side chains of the complex.

For the $\Lambda_p SR$ conformers, the two chiral ligands are of opposite chirality. Therefore, there are nine possible $\Lambda_p SR$ conformers. All these nine conformers were confirmed to be minima by DFT calculations and their geometries are given in Figure S2 in the Supporting Information. The *S* form of the ligand is kept at the front in Figure S2 for easy recognition. The theoretical predictions for the $\Lambda_p SR$ conformers are also summarized in Table 1. The calculated VA and VCD spectra of **3i**–**3ix** $\Lambda_p SR$ are presented in Figure 5. Note that the strongest VCD features at approximately 1250 cm^{-1} look very similar for all nine calculated conformers. The C=O stretching VCD features of the $\Lambda_p SR$ conformers are bisignated and with substantially lower intensities than those of $\Lambda_p SS$ and $\Delta_p SS$.

A similar conformational search procedure has been carried out for the N–P–O stereoisomers. In this case, four types of stereoisomers were expected: $\Lambda_p SS$, $\Lambda_p SR$, $\Lambda_p RS$, and $\Delta_p SS$. In general, these isomers were found to be much less stable than the O–P–O isomers. Because it has been demonstrated that the conformations associated with $CH(CH_3)_2$ produced very similar VA and VCD features in each O–P–O stereoisomeric type, the same is expected for the N–P–O stereoisomers. To be concise, only the (most) stable conformers of each of the four N–P–O types are depicted in Figure 6, together with the three of the O–P–O type for comparison. The calculated VA and VCD spectra of the four N–P–O stereoisomers are shown in Figure 7a. The calculated results for the N–P–O type are also listed in Table 1.

The O–P–O stereoisomers were predicted to be far more stable than the N–P–O ones, with the relative energy differences between the most stable N–P–O and O–P–O isomers of compound **3** being 14.66 kcal mol^{-1}. The spans of the total energies or the Gibbs free energies among the O–P–O isomers and among the N–P–O ones, on the other hand, are fairly small. The conversion of the O–P–O isomers to the N–P–O ones may, in general, be accomplished through a Berry pseudorotation with a SP transition state.[17] The possible transition state was identified and the barrier height for such a conversion was estimated to be 37.45 kcal mol^{-1} at the B3LYP/6-31G* level (see Figure S3 in the Supporting

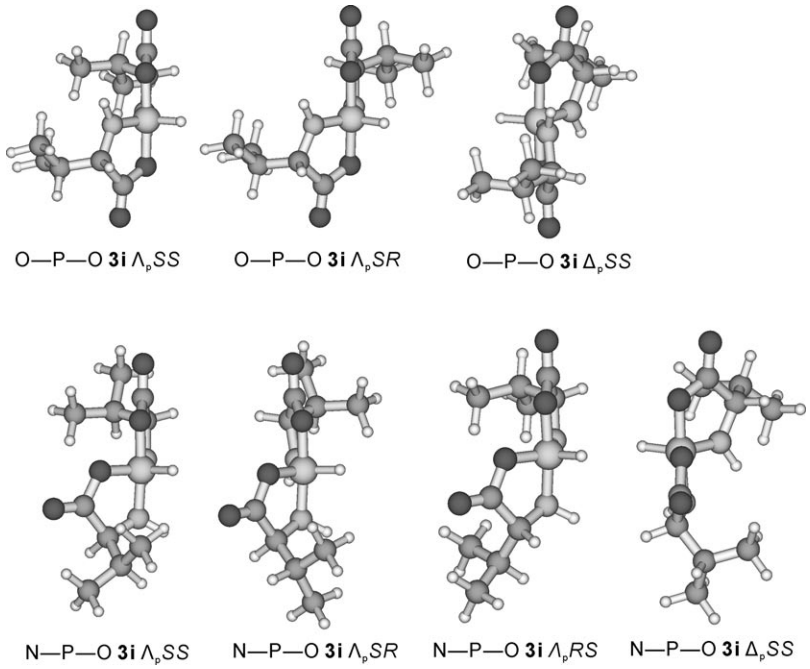

Figure 6. Optimized geometries of the seven representative structures of O–P–O $\Lambda_p SS$, $\Lambda_p SR$, $\Delta_p SS$, and N–P–O $\Lambda_p SS$, $\Lambda_p SR$, $\Lambda_p RS$, $\Delta_p SS$ stereoisomers of **3** at the B3LYP/6-311++G** level of theory.

Information). This large energy barrier indicates that the conversion between the two conformers is greatly restricted. Experimentally, we expect the main species of **3** in the $CDCl_3$ solution to be of the O–P–O type.

The calculated population-weighted VA and VCD spectra of each O–P–O type are shown in Figure 7b, together with the experimental VA and VCD spectra obtained for the diastereomeric pair of compound **3** (i.e., **3a** and **3b**) for easy comparison. One immediately notices that the calculated VA and VCD features of the O–P–O and N–P–O types significantly differ. In the N–P–O stereoisomers, because the two valine ligands bind to the P atom through either the N or O atom, this lifts the similarity of the two ligands, in contrast with the O–P–O case. As a result, the two C=O stretching frequencies become noticeably offset, producing very distinct VA and VCD signatures. Conversely, the rest of the VA and VCD features in N–P–O are also considerably affected. Because the O–P–O and the N–P–O-type complexes exhibit very different VA patterns, these two types of structural isomers can be differentiated by using their VA spectra. Clearly, the experimental VA spectra of **3a** and **3b** are consistent with a complex with an O–P–O axis. The VA spectra of the $\Lambda_p SS$, $\Delta_p SS$, and $\Lambda_p SR$ conformers containing an O–P–O axis, on the other hand, are almost identical to each other. It is, therefore, not possible to tell them apart by using VA spectroscopy. For the absolute configuration assignment, comparison of the observed and calculated VCD spectra clearly shows that the calculated spectrum of the $\Lambda_p SS$ absolute configuration most closely resembles the experimentally observed spectrum for **3a**. Not only the band positions, but also the relative intensities are well reproduced. Similarly, one can assign the absolute configuration of **3b** to $\Delta_p SS$.

To evaluate the influence of basis sets and solvents on the calculated VA and particularly on the VCD spectra, we used the aug-cc-pVDZ basis set to reoptimize the most stable $\Lambda_p SS$ conformer, O–P–O **3i** $\Lambda_p SS$, and to recalculate its VA and VCD spectra. The simulated VA and VCD spectra of these two different basis sets are summarized in Figure S4 in the Supporting Information. It can be seen that there is little difference between the calculated results by using these two different basis sets.

In general, solvents can have profound effects on the measured VA and VCD spectra. Subsequently, the effects of $CDCl_3$ on the VA and VCD spectra of O–P–O **3i** $\Lambda_p SS$ were considered. The $CDCl_3$ solvent was treated as a continuum dielectric environment with a dielectric constant of 4.9. The geometry optimizations and the frequency calculations of O–P–O **3i** $\Lambda_p SS$ were repeated by using the implicit polarizable continuum model (IPCM)[18] with B3LYP/6-311++G**. The spectra obtained with and without the IPCM consideration for **3i** $\Lambda_p SS$ are compared in Figure S5 (see the Supporting Information). The simulated spectra with IPCM are very similar to the corresponding gas-phase calculations except for some very small frequency shifts in a few of the VA bands. The inclusion of the IPCM model does not seem to improve the agreement with the experimental data. This suggests that solvent effects are negligible in this case. All further calculations presented here were, therefore, performed in the gas phase.

The assignment of **3a** to an O–P–O $\Lambda_p SS$ structure is entirely consistent with the X-ray crystallographic determination of **3a**. The calculated structural parameters of the most stable conformer **3i** $\Lambda_p SS$ by using both basis sets are given in Table S1 in the Supporting Information, together with the data obtained from the X-ray study for comparison. It can be seem that the B3LY/6-311++G** and the B3LYP/aug-cc-pVDZ calculations produced very similar structural parameters. Furthermore, all of the important X-ray structural parameters associated with the phosphorous atom are well reproduced by the calculations that use these two basis sets. Although the rotations related to τ_1 and τ_2 as indicated in Figure 1 are quenched in a solid-state structure, such rotations are possible in solution, resulting in a distribution of rotamers. Such a distribution has been modeled by using the population-weighted VA and VCD spectra as shown here,

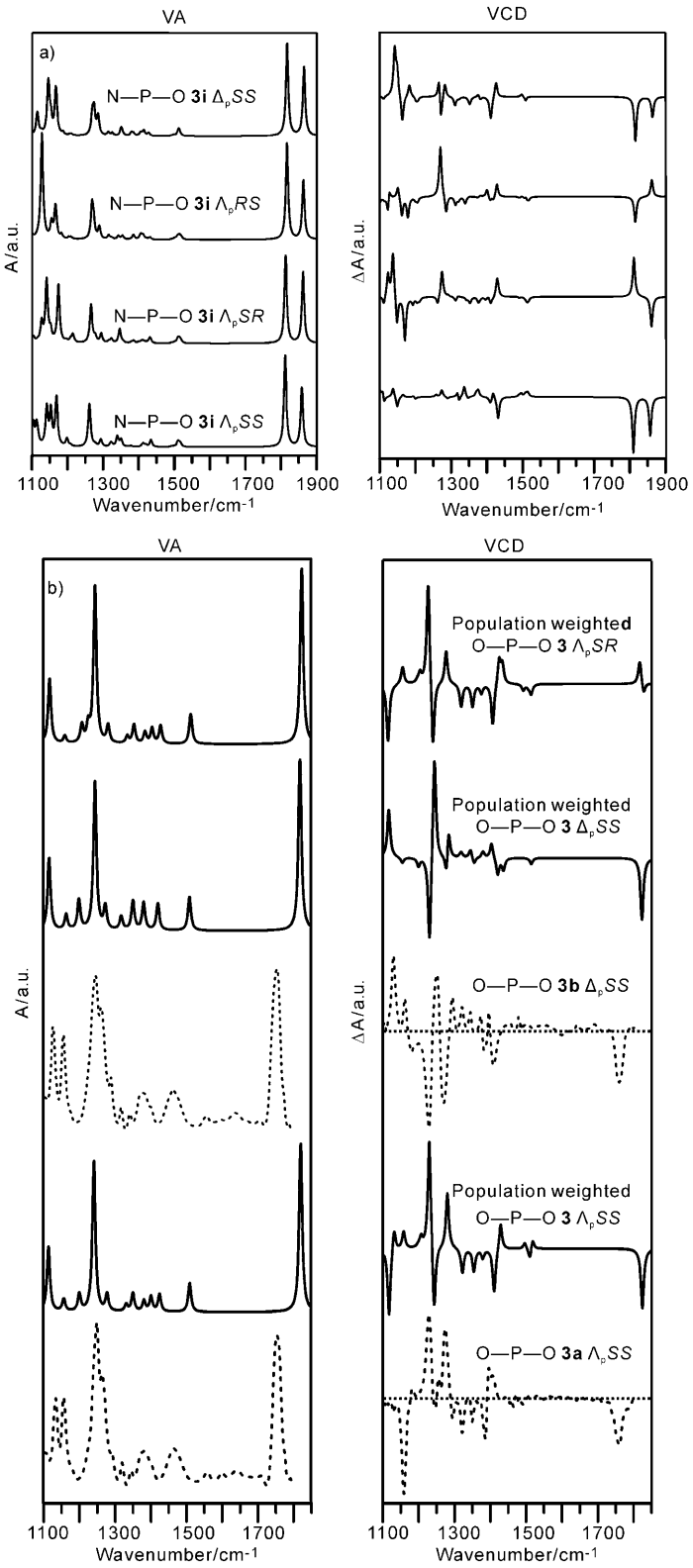

Figure 7. a) The calculated VA and VCD spectra of the four most stable N–P–O $\Lambda_p SS$, $\Lambda_p SR$, $\Lambda_p RS$, and $\Lambda_p RR$ stereoisomers of **3** at the B3LYP/6-311++G** level of theory. b) Comparison of the experimental (-----) VA (left) and VCD (right) spectra of **3a** and **3b** with the corresponding calculated population-weighted spectra (——) of the O–P–O axis $\Lambda_p SR$, $\Lambda_p SS$ and $\Delta_p SS$ stereoisomers.

although their existence does not notably influence the appearance of either the VA or the VCD spectrum.

Pentacoordinate phosphorus compounds 5 and 6: The characterization of the enantiomeric pair **5** and **6** follows the same procedure as for **3** and **4**. Compounds **5** and **6** are similar to compounds **3** and **4** except that their amino acid ligands are leucine instead of valine. The possible conformers of leucine had been previously reported by Alonso et al, who used a laser ablation molecular beam Fourier transform microwave spectrometer to detect their rotational spectra and utilized MP2 calculations to interpret the data.[19] They found that the CH_2–$CH(CH_3)_2$ side chain of leucine has nine possible conformations. Because there are two leucine ligands in each phosphorous complex, the number of possible conformations related to the orientation of the leucine chains is $9\times9=81$. Some of them, however, are redundant in the O–P–O conformers. This reduces the number to 45 possible conformations for the O–P–O $\Lambda_p SS$ type. The rotations of the CH_2–$CH(CH_3)_2$ side chain of leucine and the two most stable conformers of $\Lambda_p SS$ and $\Delta_p SS$ of **5** are shown in Figure 8. Although all of these 45 conformations

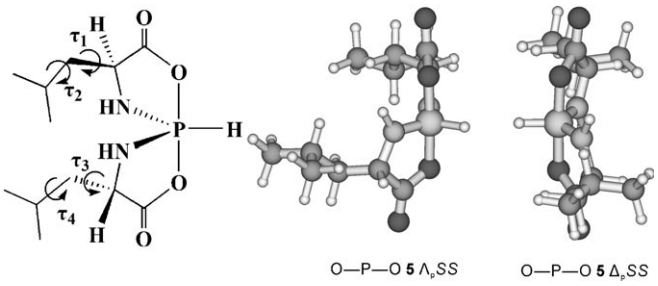

Figure 8. The rotations of the aliphatic side chain of leucine and the optimized geometries of the two most stable O–P–O $\Lambda_p SS$ and $\Delta_p SS$ stereoisomers of **5** at the B3LYP/6-311++G** level of theory.

were identified to be minima at the B3LYP/6-31G* level, only 38 of them were found stable at the B3LPY/6-311++G** level. The corresponding structures at the B3LYP/6-31G* level are shown in Figure S6 and the relative energies and Boltzmann factors with both basis sets are given in Table S2 in the Supporting Information. The VA and VCD spectra of the eight most stable conformers of the O–P–O $\Lambda_p SS$ type have been simulated and are shown in Figure 9. These eight conformers account for approximately 97% of the total population. Again, the side chain conformations play a very minor role in the appearance of the VA and VCD spectra. This conclusion echoes the one drawn from the valine ligand case discussed earlier. Similar calculations have also been performed for the O–P–O $\Delta_p SS$ type conformers. The 45 conformers identified for the O–P–O $\Delta_p SS$ type are shown in Figure S7, and the corresponding VA and VCD spectra of the eight most stable conformers are depicted in Figure S8 in the Supporting Information. Again, the rotations of the side chains have little effect on the appear-

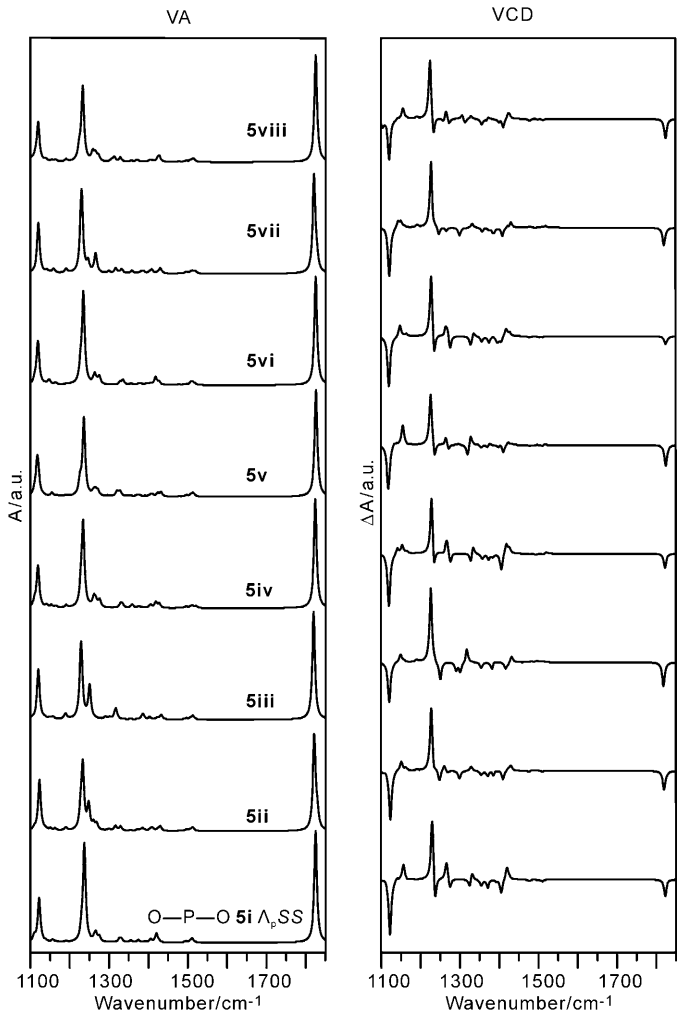

Figure 9. The calculated VA and VCD spectra of the eight most stable O–P–O $\Lambda_p SS$ conformers of **5** at the B3LYP/6-311++G** level of theory.

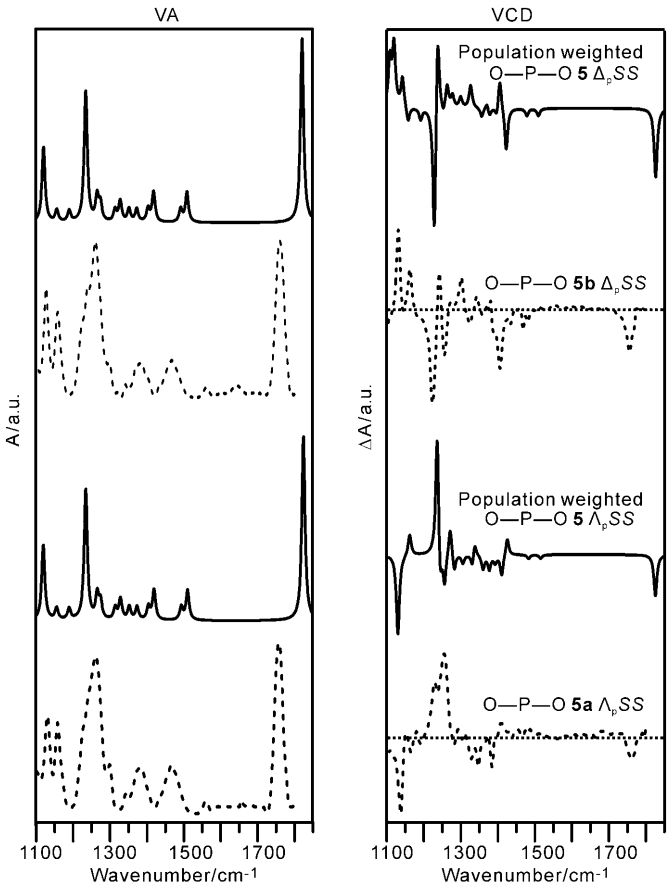

Figure 10. Comparison of the experimental (-----) VA (left) and VCD (right) spectra of **5a** and **5b** with the corresponding calculated population weighted spectra (——) of the O–P–O $\Lambda_p SS$ and $\Delta_p SS$ stereoisomers.

ance of the VA and VCD spectra. The relative energies and Boltzmann factors are summarized in Table S3 in the Supporting Information.

Finally, the population-weighted VA and VCD spectra of the O–P–O $\Lambda_p SS$ and the O–P–O $\Delta_p SS$ types are compared to the experimental spectra obtained for **5a** and **5b** in Figure 10. It can be seen that the calculated VA spectra appear to be basically the same for $\Lambda_p SS$ and $\Delta_p SS$, and the same can be said about the experimental VA spectra of **5a** and **5b**. Furthermore, the experimental VA spectra are in good agreement with the calculated ones. This confirms that the diastereomers observed contain the O–P–O axis based on the earlier discussions about the dramatic different VA spectra for the O–P–O and N–P–O-type complexes. Both **5a** and **5b** exhibit a strong negative C=O VCD signature. Because the C=O VCD features are controlled by the chirality of the leucine ligands, we assigned the absolute configurations for the two leucine ligands involved *SS* configurations. For the absolute configuration of the P center, we compared the experimental VCD features below 1500 cm^{-1} with the calculated ones. It is clear that **5a** and **5b** can be assigned to O–P–O $\Lambda_p SS$ and O–P–O $\Delta_p SS$-type configurations, respectively.

Conclusion

We have reported a combined experimental and theoretical VA and VCD study of four pentacoordinate hypervalent spirophosphoranes. The dominating conformations and the absolute configurations of these compounds in solution have been determined based on the good agreements between the experimental and simulated spectra. Both the VA and the VCD spectra demonstrate great sensitivity in discriminating between structural isomers of different axial coordination arrangements, but no (or little) sensitivity to the isomerism of the related chiral ligands. The sensitivity of different portions of the VCD spectra to the stereogenic centers located at the phosphorus atom and chiral ligands has also been investigated. This work shows that VCD spectroscopy combined with DFT calculations can be a powerful tool for determining the absolute configurations of synthetic phosphorus coordination complexes that are difficult to crystallize.

Experimental Section

Experimental methods: The samples of our studied compounds were obtained from Xiamen University, the synthetic routes of which have been were previously described.[12] The VA and VCD spectra were recorded with a Fourier transform IR spectrometer Vertex 70 (Bruker) equipped with a PMA 50 (Bruker) VCD optical bench. Samples were held in a variable path length cell with BaF_2 windows. A frequency filter with a cut off at ~1800 cm^{-1} was inserted into the beam path just before the sample cell. The spectral range of the measurements was from 1100 to 1800 cm^{-1}. Each VCD spectrum was collected with 180 min (3×60 min) and with a resolution of 4 cm^{-1}. Because the intensity of a VCD signal is typically 10^4 to 10^6 times weaker than a regular VA signal, it is sensitive to artifacts. To minimize artifacts, it is desirable to keep the absorption coefficients of most of the VA peaks in the measured frequency region between 0.2 and 0.8. An optimal experimental condition with a sample of ~0.09 M in $CDCl_3$ and a path length of 450 μm was determined. Each VA spectrum reported was obtained by subtracting the corresponding solvent spectrum that had been obtained under the same condition from the solution spectrum, whereas the VCD spectrum was obtained by taking the difference spectrum of the two enantiomeric compounds recorded under identical conditions, and then dividing it by two. The raw VCD spectra for these eight compounds are given in Figure S9 in the Supporting Information.

Calculation methods: The geometry optimizations, VA frequencies, and VA and VCD intensities for the possible conformers were performed by using the Gaussian 03 program package.[20] In this study, the B3LYP[21] hybrid functional was chosen because of its proven reliability in predicting molecular geometries and VCD intensities.[22] The 6–311++G** basis set was adopted in this study because it had been successfully used to characterize not only the band position, but also the relative intensity of the VCD peaks.[23] To facilitate comparison with the experimental data, Lorentzian line shapes with a full width at half maximum of 10 cm^{-1} were used to simulate the VA and VCD spectra. To evaluate the potential solvent effects due to $CDCl_3$, the integral equation formalism (IEF)[24] version of the IPCM[18] as implemented in Gaussian 03 program was used. The $CDCl_3$ solvent was treated as a continuum dielectric environment with a dielectric constant of 4.9.

Acknowledgements

This research was funded by the University of Alberta, the Natural Sciences and Engineering Research Council of Canada, Alberta Ingenuity, and Petro-Canada. This work was also supported by the Major Program of NSFC (No.20732004), NSFC (No.20972130), and NSFC (No. 20773098). We also gratefully acknowledge access to the computing facilities provided by the Academic Information and Communication Technology group at the University of Alberta.

[1] a) K. M. Pietrusiewicz, M. Zabłocka, *Chem. Rev.* **1994**, *94*, 1375–1411; b) R. Noyori, *Asymmetric Catalysis in Organic Synthesis*, Wiley, New York, **1994**; c) L. D. Quin, *A Guide to Organophosphorus Chemistry*, Wiley-Interscience, New York, **2000**; d) *Catalytic Asymmetric Synthesis* (Ed.: I. Ojima), Wiley-VCH, New York, **2000**; e) J. Drabowicz, P. Lyzwa, J. Omelanczuk, K. M. Pietrusiewicz, M. Mikolajczyk, *Tetrahedron: Asymmetry* **1999**, *10*, 2757–2763.

[2] a) K.-Y. Akiba, *Chemistry of Hypervalent Compounds*, Wiley-VCH, New York, **1999**; b) R. R. Homes, *Pentacoordinated Phosphorus–Structure and Spectroscopy, Vol. I and II*, ACS, Washington, **1980**; c) D. E. C. Corbridge, *Phosphorus: An Outline of Its Chemistry, Biochemistry and Technology*, 4th ed., Elsevier, Amsterdam, **1990**, Chapter 14, pp. 1233–1256; d) R. Burgada, R. Setton, *The Chemistry of Organophosphorus Compounds, Vol. 3* (Ed.: F. R. Hartley,), Wiley-Interscience, New York, **1994**, pp. 185–277.

[3] D. E. C. Corbridge, *Phosphorus, Chemistry, Biochemistry and Technology*, 4th ed., Elsevier, Amsterdam, **2000**.

[4] a) F. H. Westheimer, *Acc. Chem. Res.* **1968**, *1*, 70–78; b) S. L. Buchwald, D. H. Pliura, J. R. Knowla, *J. Am. Chem. Soc.* **1984**, *106*, 4916–4922; c) J. R. Knowles, *Annu. Rev. Biochem.* **1980**, *49*, 877–919; d) P. J. J. M. Vanool, H. M. Buck, *Recl. Trav. Chim. Pays-Bas* **1984**, *103*, 119–122; e) R. R. Holmes, *Pentacoordinated Phosphorus, Vol. 11*, ACS, Washington, **1980**, p. 87.

[5] a) R. R. Holmes, *Acc. Chem. Res.* **2004**, *37*, 746–753; b) R. R. Holmes, *Acc. Chem. Res.* **1998**, *31*, 535–542.

[6] a) K. C. K. Swamy, N. S. Kumar, *Acc. Chem. Res.* **2006**, *39*, 324–333; b) N. S. Kumar, K. P. Kumar, K. V. P. P. Kumar, P. Kommana, J. J. Vittal, K. C. K. Swamy, *J. Org. Chem.* **2004**, *69*, 1880–1889.

[7] N. V. Timosheva, A. Chandrasekaran, R. R. Holmes, *J. Am. Chem. Soc.* **2005**, *127*, 12474–12475.

[8] H. Fu, J. H. Xu, R. J. Wang, Z. Z. Chen, G. Z. Tu, Q. Z. Wang, Y. F. Zhao, *Phosphorus, Sulfur. Silicon. Relat. Elem.* **2003**, *178*, 1963–1971.

[9] H. Fu, Z. L. Li, Y. F. Zhao, G. Z. Tu, *J. Am. Chem. Soc.* **1999**, *121*, 291–295.

[10] a) S. D. Lahiri, G. F. Zhang, D. Dunaway-Mariano, K. N. Allen, *Science* **2003**, *299*, 2067–2071; b) G. M. Blackburn, N. H. Williams, S. J. Gamblin, S. J. Smerdon, *Science* **2003**, *301*, 1184c; c) I. Leiros, S. McSweeney, E. Hough, *J. Mol. Biol.* **2004**, *339*, 805–820; d) N. H. Williams, *Biochim. Biophys. Acta* **2004**, *1697*, 279–287; e) A. C. Hengge, I. Onyido, *Curr. Org. Chem.* **2005**, *9*, 61–74; f) W. W. Cleland, A. C. Hengge, *Chem. Rev.* **2006**, *106*, 3252–3278; g) A. Wittinghofer, *Trends Biochem. Sci.* **2006**, *31*, 20–23; h) I. Catrina, P. J. O'Brien, J. Purcell, I. Nikolic-Hughes, J. G. Zalatan, A. C. Hengge, D. Herschlag, *J. Am. Chem. Soc.* **2007**, *129*, 5760–5765; i) E. Marcos, R. Crehuet, J. M. Anglada, *J. Chem. Theory Comput.* **2008**, *4*, 49–63.

[11] a) H. Fu, G. Z. Tu, Z. L. Li, Y. F. Zhao, R. Q. Zhang, *J. Chem. Soc. Perkin Trans.* **1997**, 2021–2022; b) L. Yu, Z. Liu, H. Fang, Q. L. Zeng, Y. F. Zhao, *Amino Acids* **2005**, *28*, 369–372.

[12] J. B. Hou G. Tang, J. N. Guo, Y. Liu, H. Zhang, Y. F. Zhao, *Tetrahedron: Asymmetry* **2009**, *20*, 1301–1307.

[13] a) T. A. Keiderling, *Nature* **1986**, *322*, 851–852; b) K. Nakanishi, N. Berova, R. W. Woody, *Circular Dichroism: Principles and Applications*, Wiley-VCH, Weinheim, **2000**; c) R. A. G. D. Silva, J. Kubelka, P. Bour, S. M. Decatur, T. A. Keiderling, *Proc. Natl. Acad. Sci. USA* **2000**, *97*, 8318–8323; d) J. H. Choi, M. Cho, *J. Chem. Phys.* **2004**, *120*, 4383–4392; e) G. Shanmugam, P. L. Polavarapu, *J. Am. Chem. Soc.* **2004**, *126*, 10292–10295; f) J. Hilario, J. Kubelka, T. A. Keiderling, *J. Am. Chem. Soc.* **2003**, *125*, 7562–7574; g) F. Eker, X. L. Cao, L. Nafie, R. Schweitzer-Stenner, *J. Am. Chem. Soc.* **2002**, *124*, 14330–14341.

[14] a) L. D. Barron, *Molecular Light Scattering and Optical Activity*, 2nd ed., Cambridge University Press, New York, **2004**; b) T. Brotin, D. Cavagnat, J. P. Dutasta, T. Buffeteau, *J. Am. Chem. Soc.* **2006**, *128*, 5533–5540; c) P. J. Stephens, J. J. Pan, K. Krohn, *J. Org. Chem.* **2007**, *72*, 7641–7649; d) A. Muranaka, M. Shibahara, M. Watanabe, T. Matsumoto, T. Shinmyozu, N. Kobayashi, *J. Org. Chem.* **2008**, *73*, 9125–9128; e) H. Izumi, A. Ogata, L. A. Nafie, R. K. Dukor, *J. Org. Chem.* **2009**, *74*, 1231–1236; f) G. Tarczay, G. Magyarfalvi, E. Vass, *Angew. Chem.* **2006**, *118*, 1807–1809; *Angew. Chem. Int. Ed.* **2006**, *45*, 1775–1777; g) M. Urbanová, V. Setnicka, F. J. Devlin, P. J. Stephens, *J. Am. Chem. Soc.* **2005**, *127*, 6700–6711; h) K. Monde, T. Taniguchi, N. Miura, *J. Am. Chem. Soc.* **2004**, *126*, 9496–9497.

[15] a) S. G. Stepanian, I. D. Reva, E. D. Radchenko, L. Adamowicz, *J. Phys. Chem. A* **1999**, *103*, 4404–4412; b) S. Mondal, D. S. Chowdhuri, S. A. Ghosh, S. Dalai, *THEOCHEM* **2007**, *810*, 81–89; c) R. Jacob, G. Fischer, *J. Phys. Chem. A* **2003**, *107*, 6136–6143.

[16] a) R. Schweitzer-Stenner, *Vib. Spectrosc.* **2006**, *42*, 98–117; b) R. Schweitzer-Stenner, F. Eker, K. Griebenow, X. L. Cao, L. A. Nafie, *J. Am. Chem. Soc.* **2004**, *126*, 2768–2776.

[17] a) H. Nakazawa, K. Kawamura, T. Ogawa, K. Miyoshi, *J. Organomet. Chem.* **2002**, *646*, 204–211; b) S. Kojima, K. Kajiyama, M. Nakamoto, S. Matsukawa, K. Akiba, *Eur. J. Org. Chem.* **2006**, 218–234.

[18] a) J. Tomasi, M. Persico, *Chem. Rev.* **1994**, *94*, 2027–2094; b) C. Cramer, D. Truhlar, *Chem. Rev.* **1999**, *99*, 2161–2200.

[19] E. J. Cocinero, A. Lesarri, J. U. Grabow, J. C. Lopez, J. L. Alonso, *ChemPhysChem* **2007**, *8*, 599–604.

[20] Gaussian 03, Revision B.05, M. J. Frisch, G. W. Trucks, H. B. Schlegel, G. E. Scuseria, M. A. Robb, J. R. Cheeseman, J. A. Montgomery, Jr., T. Vreven, K. N. Kudin, J. C. Burant, J. M. Millam, S. S. Iyengar, J. Tomasi, V. Barone, B. Mennucci, M. Cossi, G. Scalmani, N. Rega, G. A. Petersson, H. Nakatsuji, M. Hada, M. Ehara, K. Toyota, R. Fukuda, J. Hasegawa, M. Ishida, T. Nakajima, Y. Honda, O. Kitao, H. Nakai, M. Klene, X. Li, J. E. Knox, H. P. Hratchian, J. B. Cross, V. Bakken, C. Adamo, J. Jaramillo, R. Gomperts, R. E. Stratmann, O. Yazyev, A. J. Austin, R. Cammi, C. Pomelli, J. Ochterski, P. Y. Ayala, K. Morokuma, G. A. Voth, P. Salvador, J. J. Dannenberg, V. G. Zakrzewski, S. Dapprich, A. D. Daniels, M. C. Strain, O. Farkas, D. K. Malick, A. D. Rabuck, K. Raghavachari, J. B. Foresman, J. V. Ortiz, Q. Cui, A. G. Baboul, S. Clifford, J. Cioslowski, B. B. Stefanov, G. Liu, A. Liashenko, P. Piskorz, I. Komaromi, R. L. Martin, D. J. Fox, T. Keith, M. A. Al-Laham, C. Y. Peng, A. Nanayakkara, M. Challacombe, P. M. W. Gill, B. G. Johnson, W. Chen, M. W. Wong, C. Gonzalez and J. A. Pople, Gaussian, Inc., Wallingford, CT, **2003**.

[21] a) A. D. Becke, *J. Chem. Phys.* **1993**, *98*, 5648–5652; b) C. T. Lee, W. T. Yang, R. G. Parr, *Phys. Rev. B-Condens. Matter Mater. Phys.* **1988**, *37*, 785–789.

[22] a) P. J. Stephens, F. J. Devlin, C. F. Chabalowski, M. J. Frisch, *J. Phys. Chem.* **1994**, *98*, 11623–11627; b) T. Brotin, D. Cavagnat, J.-P. Dutasta, T. Buffeteau, *J. Am. Chem. Soc.* **2006**, *128*, 5533–5540; c) T. A. Martinek, I. M. Mándity, L. Fülöp, G. K. Tóth, E. Vass, M. Hollósi, E. Forró, F. Fülöp, *J. Am. Chem. Soc.* **2006**, *128*, 13539–13544; d) D. Cavagnat, L. Lespade, T. Buffeteau, *J. Phys. Chem. A* **2007**, *111*, 7014–7021; e) H. Izumi, A. Ogata, L. A. Nafie, R. K. Dukor, *J. Org. Chem.* **2009**, *74*, 1231–1236; f) T. B. Freedman, X. L. Ca, Z. Luz, H. Zimmermann, R. Poupko, L. A. Nafie, *Chirality* **2008**, *20*, 673–680.

[23] a) E. Debie, P. Bultinck, W. Herrebout, B. van der Veken, *Phys. Chem. Chem. Phys.* **2008**, *10*, 3498–3508; b) J. T. He, A. G. Petrovic, P. L. Polavarapu, *J. Phys. Chem. B* **2004**, *108*, 20451–20457; c) J. T. He, A. Petrovich, P. L. Polavarapu, *J. Phys. Chem. A* **2004**, *108*, 1671–1680; d) K. K. Lee, K. I. Oh, H. Lee, C. Joo, H. Han, M. Cho, *ChemPhysChem* **2007**, *8*, 2218–2226.

[24] E. Cancès, B. Mennucci, J. Tomasi, *J. Chem. Phys.* **1997**, *107*, 3032–3041.

Received: September 10, 2009
Published online: January 14, 2010

